J. Cell. Mol. Med. Vol 12, No 6A, 2008 pp. 2350-2361

Resveratrol enhances GLUT-4 translocation to the caveolar lipid raft fractions through AMPK/Akt/eNOS signalling pathway in diabetic myocardium

S. Varma Penumathsa, [a, c] M. Thirunavukkarasu, [a] L. Zhan, [a] G. Maulik, [b]
V. P. Menon, [c] D. Bagchi, [d] N. Maulik [a]

[a] *Molecular Cardiology and Angiogenesis Laboratory, Department of Surgery, University of Connecticut Health Center, Farmington, CT, USA*
[b] *Department of Thoracic Surgery, Harvard Medical School, Boston, MA, USA*
[c] *Department of Biochemistry and Biotechnology, Annamalai University, TN, India*
[d] *Interhealth Research Center, Benicia, CA, USA*

Received: July 16, 2007; Accepted: January 23, 2008

Abstract

Homeostasis of blood glucose by insulin involves stimulation of glucose uptake by translocation of glucose transporter Glut-4 from intracellular pool to the caveolar membrane system. In this study we examined resveratrol (RSV)-mediated Glut-4 translocation in the streptozotocin (STZ)-induced diabetic myocardium. The rats were randomized into three groups: Control (Con), Diabetes Mellitus (DM) (STZ 65 mg/kg b.w., i.p.) & DM + RSV (2.5 mg/kg b.wt. for 2 weeks orally) (RSV). Isolated rat hearts were used as per the experimental model. RSV induced glucose uptake was observed *in vitro* with H9c2 cardiac myoblast cells. Decreased blood glucose level was observed after 30 days (375 mg/dl) in RSV-treated rats when compared to DM (587 mg/dl). Treatment with RSV demonstrated increased Adenosine Mono Phosphate Kinase (AMPK) phosphorylation compared to DM. Lipid raft fractions demonstrated decreased expression of Glut-4, Cav-3 (0.4, 0.6-fold) in DM which was increased to 0.75- and 1.1-fold on RSV treatment as compared to control. Increased Cav-1 expression (1.4-fold) in DM was reduced to 0.7-fold on RSV treatment. Increased phosphorylation of endothelial Nitric Oxide Synthase (eNOS) & Akt was also observed in RSV compared to DM ($P < 0.05$). Confocal microscopy and co-immunoprecipitation studies demonstrated decreased association of Glut-4/Cav-3 and increased association of Cav-1/eNOS in DM as compared to control and converse results were obtained on RSV treatment. Our results suggests that the effect of RSV is non-insulin dependent and triggers some of the similar intracellular insulin signalling components in myocardium such as eNOS, Akt through AMPK pathway and also by regulating the caveolin-1 and caveolin-3 status that might play an essential role in Glut-4 translocation and glucose uptake in STZ- induced type-1 diabetic myocardium.

Keywords: diabetic • ischaemia/reperfusion • caveolin • AMPK • eNOS • Akt • Glut-4

Introduction

The regulation of glucose uptake and its subsequent utilization is critical for the maintenance of glucose homeostasis. It is well established that glucose uptake is controlled by glucose transporter (Glut-4) in the plasma membrane and the Glut-4 translocation to the membrane seems to be dependent on insulin-mediated signalling pathways. Adipocytes of streptozotocin (STZ) induced diabetic rats demonstrated reduction in insulin-stimulated glucose transport function and cellular Glut-4 content [1] and evidences show that the change in the glucose transporter content is more specific for Glut-4 [2]. It was also reported that both Glut-4 transport and content increase after insulin treatment [1, 2]. Dilated cardiomyopathy which is one of the major complications during diabetes and it is characterized by depletion of adenosine

*Correspondence to: Nilanjana MAULIK, Ph.D,
Molecular Cardiology and Angiogenesis Laboratory
Department of Surgery
University of Connecticut Health Center
263 Farmington Avenue, Farmington, CT 06030-1110, USA.
Tel.: (86 0) 67 9-28 57
Fax: (86 0) 67 9-28 25
E-mail: nmaulik@neuron.uchc.edu

doi:10.1111/j.1582-4934.2008.00251.x

triposphate (ATP) stores is a consequence of impaired insulin glucose uptake [3]. Insulin, a major regulator of glucose metabolism increases glucose transport by stimulating insertion of Glut-4 from intracellular compartment to the cell surface [4] and further transition of Glut-4 to the plasma membrane fraction enriched by the caveolae [5]. Caveolae are small membrane invaginations on the surface of the cells that participate in membrane trafficking, sorting, transport and signal transduction. These caveolae are enriched in sphingolipids and cholesterol and form lipid rafts in the presence of structural proteins, the caveolins that serve as a marker for the caveolae [6, 7]. Mammalian caveolin family proteins caveolin-1, 2 and 3 (Cav-1, 2 & 3) were found to be the major components of caveolae [8]. Cav-3 or M-caveolin is expressed in the muscle where as caveolin-1 is expressed in endothelial cells [9, 10]. Bucci *et al*. has shown that caveolin-1 serves as a primary structural component of caveolae and acts like a physiological inhibitor of eNOS [11] and further demonstrated that caveolin-1 expression is up-regulated in diabetic non-obese diabetic (NOD) mice [11]. Both exercise and insulin-mediated glucose uptake was found to be stimulated by nitric oxide [12, 13, 14]. AMPK, a serine–threonine kinase was shown to play an important role in regulation of cellular metabolism and as a mediator of glucose metabolism [15]. Chen *et al*. have demonstrated that activated AMPK phosphorylates eNOS both *in vitro* and during ischaemia in rat hearts [16] and Li *et al*. has shown the role of nitric oxide in AMPK-mediated glucose uptake and Glut-4 translocation [17]. In the same study Li *et al*. have also demonstrated that a relatively low concentration of nitric oxide donors stimulated Glut-4 translocation and increased glucose uptake in isolated heart papillary muscles [17]. We have shown recently that resveratrol (RSV) (a polyphenolic compound present in red wine) treatment increased myocardial function as well as reduced blood glucose level that may be mediated through nitric oxide [18]. We have also reported that RSV-induced Akt-/eNOS-mediated protection in the hypercholesterolaemic ischaemic myocardium [19]. Previous reports also demonstrated that RSV enhances nitric oxide production in endothelial cells [20] as well as in the heart [21]. It possesses many other biologic activities, including an oestrogenic activity [22], antioxidant activity [23], an anti-inflammatory function [24], and a cancer chemopreventive property [25]. In conjunction with the previous reports, in the present study we investigated the mechanism involved in RSV-mediated regulation in glucose levels in STZ-induced diabetic rats. We have also reported that ischaemic preconditioning-mediated Glut-4 translocation is mediated by differential activation of caveolins, eNOS and Akt that helps in translocation of Glut-4 vesicles [26] to the plasma membrane. Hence, in the present study we investigated the effect of RSV on glucose homeostasis in STZ-induced diabetic rats in vivo as well as RSV-mediated glucose uptake in H9c2 cells *in vitro*. In our present study, we demonstrated for the first time that RSV-induced Glut-4 translocation to the lipid rich fractions and its association with caveolin-3 may be mediated by increased activation of AMPK, Akt, eNOS and decreased association of Cav-1/eNOS resulting in glucose homeostasis in diabetic myocardium.

Materials and methods

Animals

This study was performed in accordance with the principles of laboratory animal care formulated by the National Society for Medical Research and the *Guide for the Care and Use of Laboratory Animals* prepared by the National Academy of Sciences and published by the National Institutes of Health (Publication No. 85-23, revised 1985). The experimental protocol was examined and approved by the Institutional Animal Care Committee of the Connecticut Health Center (Farmington, CT).

Experimental protocol

All animals used in the study received humane care and treatment. Male Sprague Dawley rats (275–300 g) were used for the study. Diabetes was induced in the animals by a one time intraperitoneal administration of streptozocin (STZ; Sigma, St Louis, MO) at a dosage of 65 mg/kg in citrate buffer. Control rats received an equal volume of citrate buffer (i.p.). Blood was drawn from the rats by tail snip, and glucose levels were measured using glucose monitoring system (Thera Sense, Inc. Alameda, CA, USA) after 5 days of STZ administration. Rats with blood glucose concentrations $\geq$300 mg/dl were considered to be diabetic. Rats were randomly divided into three groups (n = 12 in each group): (*i*) Non-diabetic rats (control); (*ii*) Diabetic rats (diabetes mellitus [DM]); (*iii*) DM+RSV (rats were treated with 2.5 mg / kg body weight of RSV for 2 weeks orally). After the treatment period the animals were sacrificed and the hearts were excised and used for isolation of lipid raft fractions (n = 6) and immunohistochemical analysis (n = 6) respectively.

Isolated heart preparation (baseline sample preparation)

Rats were given an intraperitoneal bolus of heparin (500 IU/kg) and were anaesthetized by the intraperitoneal administration of pentobarbital sodium (80 mg/kg, Abbot, Baxter Health Care, Deep Field, IL). The hearts were perfused for 3 min. in langendorff mode for baseline samples to clear off the blood as published earlier by Thirunavukkarasu *et al*.; 2007 [18]. After the experimental protocol the left ventricular samples were flash frozen for lipid raft fraction isolation and Western blot analysis. Another set of animals was used for immunohistochemical analysis.

Cell Culture and 2-deoxy[^{3}H]glucose uptake

H9c2 cells were maintained in Dulbeccoís modified Eagleís medium (DMEM). Glucose uptake was assayed by accumulation of 2-deoxy[^{3}H]glucose according to Kotani *et al*. [27]. In brief, confluent H9c2 cells in 12-well plates were washed twice with Dulbecco's Buffer (140 mM NaCl, 2.7 mM KCl, 1 mM $CaCl_2$, 1.5 mM KH_2PO_4, 8 mM Na_2HPO_4 pH 7.4, 0.5 mM $MgCl_2$) containing 0.2% bovine serum albumin (BSA) and incubated in DB buffer for 30 min. at 37°C. Insulin was added

to a final concentration 100 nM and cells were further incubated for 30 min. that was used as the positive control. In separate wells, RSV was added in concentrations of 25, 50 and 100 μM. The 50-μM dose was found to be effective and this dose was further used to determine the time-point of glucose uptake and 8 hrs of treatment was found to be effective. Finally, DB buffer containing 0.2% BSA and 0.05 mM 2-deoxy[^{3}H]glucose (0.5 μCi) was added to each well and after 5 min. of incubation, cells were washed three times with ice-cold PBS and solubilized with 0.1% (w/v) SDS. The radioactivity incorporated into the cells was measured with a liquid scintillation counter.

Isolation of caveolin-rich(lipid raft) fractions

100–105 mg of tissue was homogenized in 2 ml of sucrose buffer (250 mM sucrose, 25 mM Tris (pH 7.4), 2 mM ethylenediaminetetraacetic acid [EDTA], 150 mM NaCl, 1% Triton X-100, and protease inhibitor cocktail) according to the modified protocol of Liu *et al.* [28] using a Polytron homogenizer and the procedure was followed according as shown earlier by Koneru *et al.* [26]. In brief, 5%, 30% and 80% sucrose solution were made in TNE (Tris, NaCl and EGTA). The lysate was passed through a 23 g needle and was sonicated. Following sonication, 2 ml of 80% sucrose was added and mixed to make the sucrose concentration to 40%. On the top of this, 4 ml of 30% sucrose was added followed by 4 ml of 5% sucrose solution. Thus, the total volume was made to 12 ml. The tubes containing sucrose gradient was centrifuged at 33,000 rpm for 17 hrs. Following centrifugation, the gradient was separated into 12 fractions of 1 ml each. Equal amount of protein was loaded for all the groups to perform Western blot analysis.

Immunoprecipitation for Cav-1/eNOS and Cav-3/GLUT-4 association

Caveolin-rich fractions (*fractions 4–6*) were used for immunoprecipitation. Immunoprecipitation was performed with protein-A and protein-G Sepharose beads from Amersham Biosciences (Piscataway, NJ) using a polyclonal antibody against Cav-1 and Cav-3 monoclonal antibody from Santa Cruz Biotechnology (Santa Cruz, CA). The procedure was carried out according to manufacturer's protocol. The caveolin-rich fractions (*fractions 4–6*) were immunoprecipitated with Cav-1 and Cav-3, which were re-blotted with eNOS and GLUT-4, respectively.

Western blot analysis for p-AMPK, AMPK, Cav-1, Cav-3, GLUT-4, p-eNOS, eNOS and p-Akt and Akt

To quantify the amount of Cav-1, Cav-3, GLUT-4 and phosphorylated and non-phosphorylated AMPK, eNOS and Akt in the cytosolic and lipid raft fractions, standard SDS-PAGE Western blot analysis was performed with the use of polyacrylamide electrophoretic gels (7%, 10% and 12%; acrylamide-to-bis ratios depending on the molecular weight of the proteins) as described previously [19, 26]. The antibodies were purchased (Cell Signaling Technology, Danvers, MA; Abcam, Cambridge, MA; and Santa Cruz Biotechnology) and were used at manufacturer-recommended dilutions.

Table 1 Effect of resveratrol treatment on blood glucose levels in streptozotocin-induced diabetic rats

Groups	Final (mg/dl) after 30 days
Control	90±2.3
Diabetic	587±43.4*
Diabetic + Resveratrol	375±18.6†

Immunohistochemistry of Caveolin-1/3, Caveolin-1/eNOS and Caveolin-3/Glut-4

Paraffin-embedded tissue sections of 4 μm thick were used for immunohistochemical analysis. The sections were deparaffinized using histoclear solution, 100%, 90%, 80% and 70% ethanol followed by phosphate buffered saline (PBS) wash. Each step was carried for 5 min. Slides were placed in boiling antigen retrieval buffer for 15 min. and was then allowed to cool at room temperature for 20 min. Again, the slides were rinsed in PBS. The sections were rinsed with 0.5% BSA in PBS for 20 min. The slides were blocked in 10% normal donkey serum with 1% BSA in PBS for 2 hrs. For Glut-4, the sections were rinsed and blocked with 0.4% triton-X 100 along with BSA. Following blocking, the sections was incubated overnight with primary antibodies for Cav-1 (SantaCruz Biotechnology) Cav-3, eNOS (BD Pharmingen, San Diego, CA) and Glut-4 (Chemicon International, Temecula, CA) diluted with 1% BSA in PBS overnight at room temperature. All primary antibodies were diluted at 1:100 ratios. After overnight incubation the sections were washed in PBS. The sections were rinsed with 0.5% BSA in PBS for three times for 5 min. each. The sections were incubated with secondary antibodies Alexa flour 555 anti-rabbit (for Cav-1), anti-goat (for Glut-4) and Alexa flour 488 antimouse (for Cav-3 and eNOS) from Invitrogen, Eugene, Oregon,USA The secondary antibodies were diluted with 1% BSA in PBS. The sections were incubated in secondary for 2 hrs. After incubation the sections were rinsed in PBS and mounted with citifluor mounting medium (Vector Laboratories Inc, Burlingame, CA) as described previously [26]. The sections were observed and pictures were taken using Confocal 410 microscope.

Statistical significance

Results are expressed as mean ± standard deviation of the mean (±SD). Differences between groups were tested for statistical significance by one-way analysis of variance (ANOVA) followed by Bonferoniís correction, to test for any differences between the mean values of all groups.

Results

Effect of resveratrol on glucose levels

In our present study, as we have shown earlier [18] blood glucose level (n = 12 in each group) was significantly increased in the diabetic rats when compared to non-diabetic rats (90 mg/dl) and reduced on treatment with RSV. RSV therapy decreased the blood glucose level significantly in RSV group (375 mg/dl) when compared to DM group (>587mg/dl) after 30 days (Table 1).

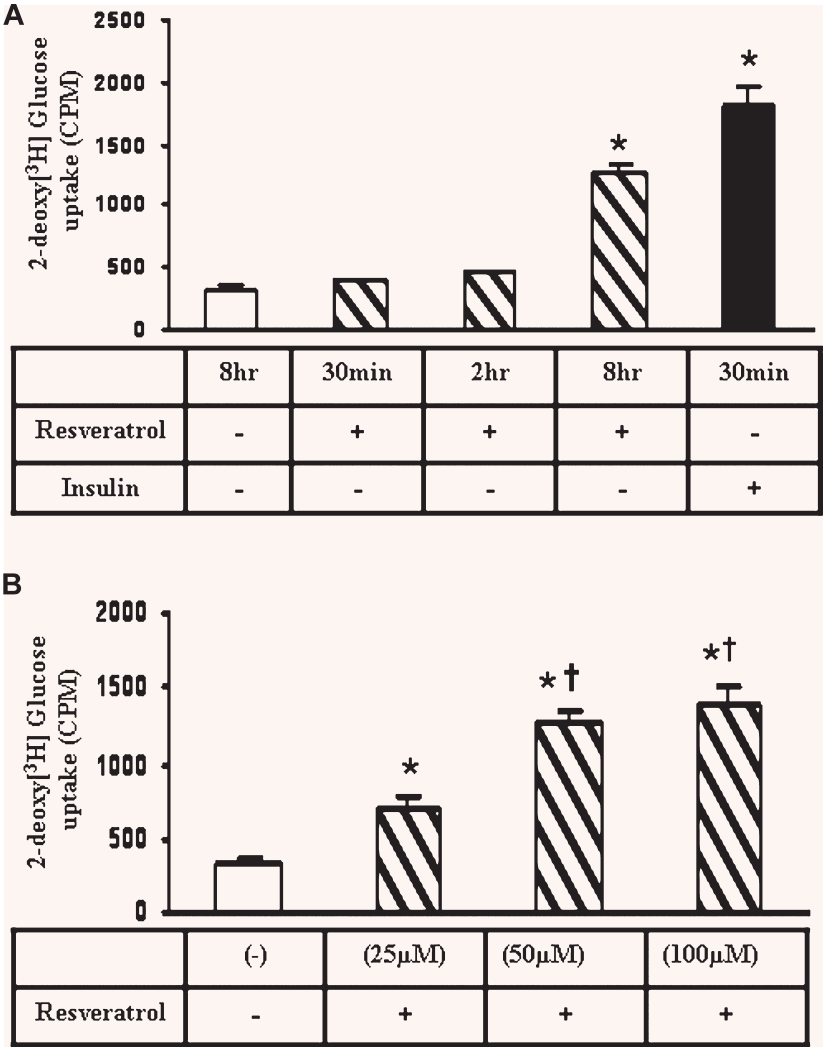

Fig. 1 (**A**) Graph represents the resveratrol (RSV) (50 μm) mediated 2-deoxy[^{3}H]glucose uptake in H9c2 cardiac myoblast cells in a time dependent manner. Insulin treatment was used as the positive control. $^*P < 0.05$ represent significant difference in comparison with control or non-treated cells. (**B**) Graph represents the resveratrol-mediated 2-deoxy[^{3}H]glucose uptake in H9c2 cardiac myoblast cells in a dose dependent manner. 50 μM RSV treatment has shown significant increase when compared to 25 μM but no significant difference was observed between 50 μM and 100 μM. $^*P < 0.05$ represent significant difference in comparison with control or non-treated cells. $^\dagger P < 0.05$ represent significant difference in comparison with 25 μM resveratrol-treated cells.

Effect of resveratrol on 2-deoxy[^{3}H] glucose uptake

We examined the dosage and time-dependent effect of RSV on glucose (2-deoxy[^{3}H] glucose) uptake in H9c2 cells as described previously in the method section. We have observed increased glucose uptake in RSV-treated cells when compared to the normal control. There was no significant increase in glucose uptake after 30 min. or 2 hrs of RSV treatment. However, we have observed a significant increase (3.6-fold) in the glucose uptake after 8 hrs of treatment with RSV (50 μm) as compared to the normal control. Cells treated with insulin (100 nM, positive control) showed a significant increase (4.9-fold) in the glucose uptake as early as 30 min. of treatment (Fig. 1A). Insulin action was much faster as compared to RSV even at earlier time-points, but when incubated for longer time no significant difference was observed so we have used shorter time-point (30 min.). Furthermore, we have observed a significant increase in the glucose uptake with increasing RSV concentrations or dose as compared to the normal control. There was a significant increase (3.9-fold) in glucose uptake at 50-μM concentration of RSV when compared to the normal control. However, a further increase in concentration of RSV treatment (100 μM) did not show any significant difference (3.9-fold versus 4.2-fold) in glucose uptake with respect to the 50 μM RSV-treated cells (Fig. 1B).

Effect of resveratrol on phosphorylation of Akt and AMPK levels

Decreased phosphorylation of Akt was observed in the diabetic group as compared to control group. RSV treatment increased

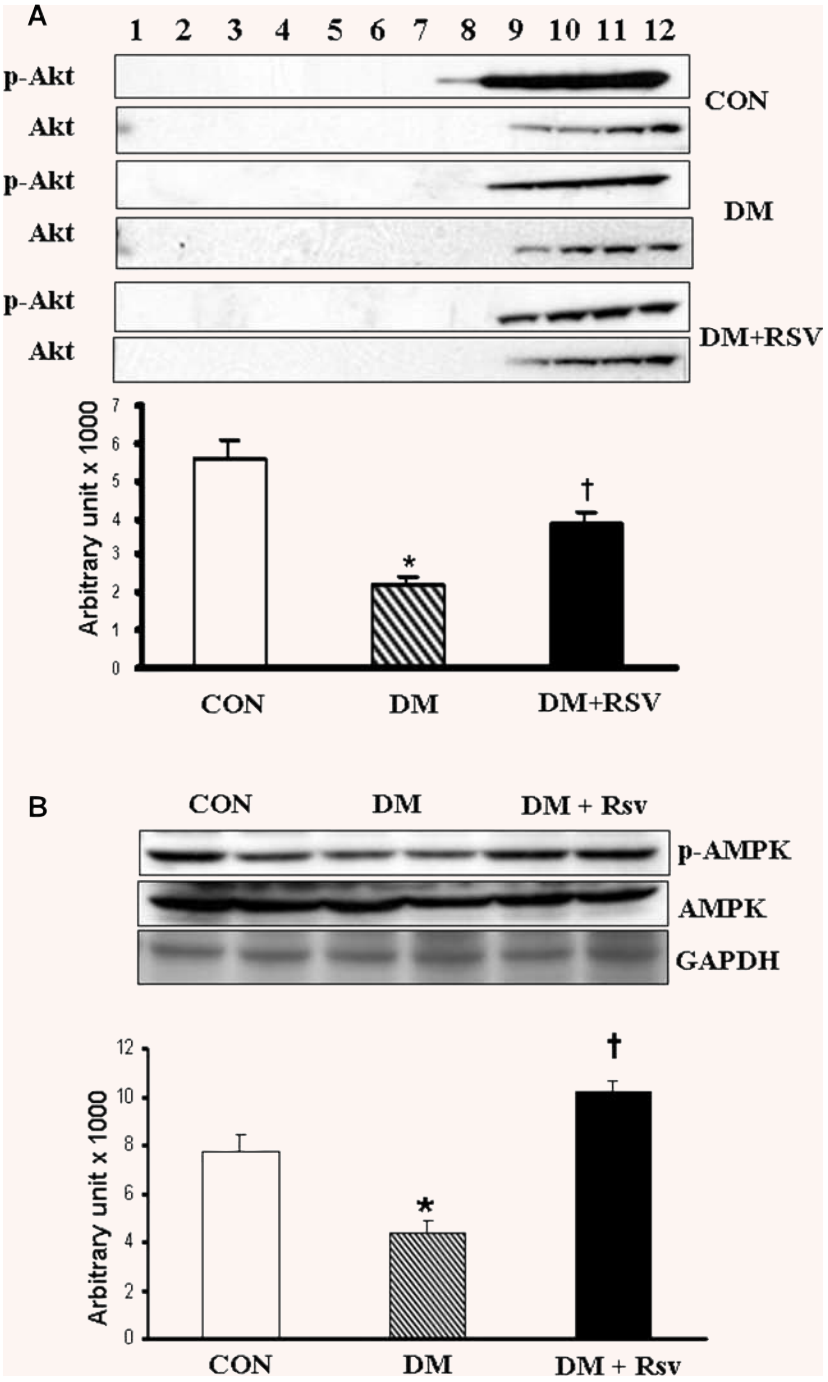

Fig. 2 (**A**) Western blot represents the p-Akt protein expression in caveolin/lipid raft fractions in control, diabetes mellitus (DM) and DM+RSV groups. Density value of p-Akt bands were normalized to level of Akt and expressed relative to control. Fractions 4–6 represent the membrane fractions and 8–12 represent the cytosolic fractions. (**B**) Protein expression levels of p-AMPK in cytosolic fractions of control, DM and DM+RSV groups. Density value of p-AMPK bands were normalized to level of AMPK and expressed relative to control. GAPDH was used as the loading control. n = 4 times repeated experiments with equivalent results. Graphs represent the quantitative expression between the groups. $^{*}P < 0.05$ represent significant difference compared with control. $^{\dagger}P < 0.05$ represent significant difference compared with DM.

the phosphorylation of Akt (2-fold) as compared to DM group (Fig. 2A). The phosphorylation of AMPK was found to be reduced in diabetic group (0.5-fold) as compared to non-diabetic control. RSV treatment increased the phosphorylation of AMPK (2.3-fold) as compared to the non-treated diabetic control. Density value of p-AMPK bands were normalized with the AMPK value and expressed relative to control. Glyceraldehyde Phosphate Dehydrogenase (GAPDH) was used as the loading control and no significant difference was observed between the groups (Fig. 2B).

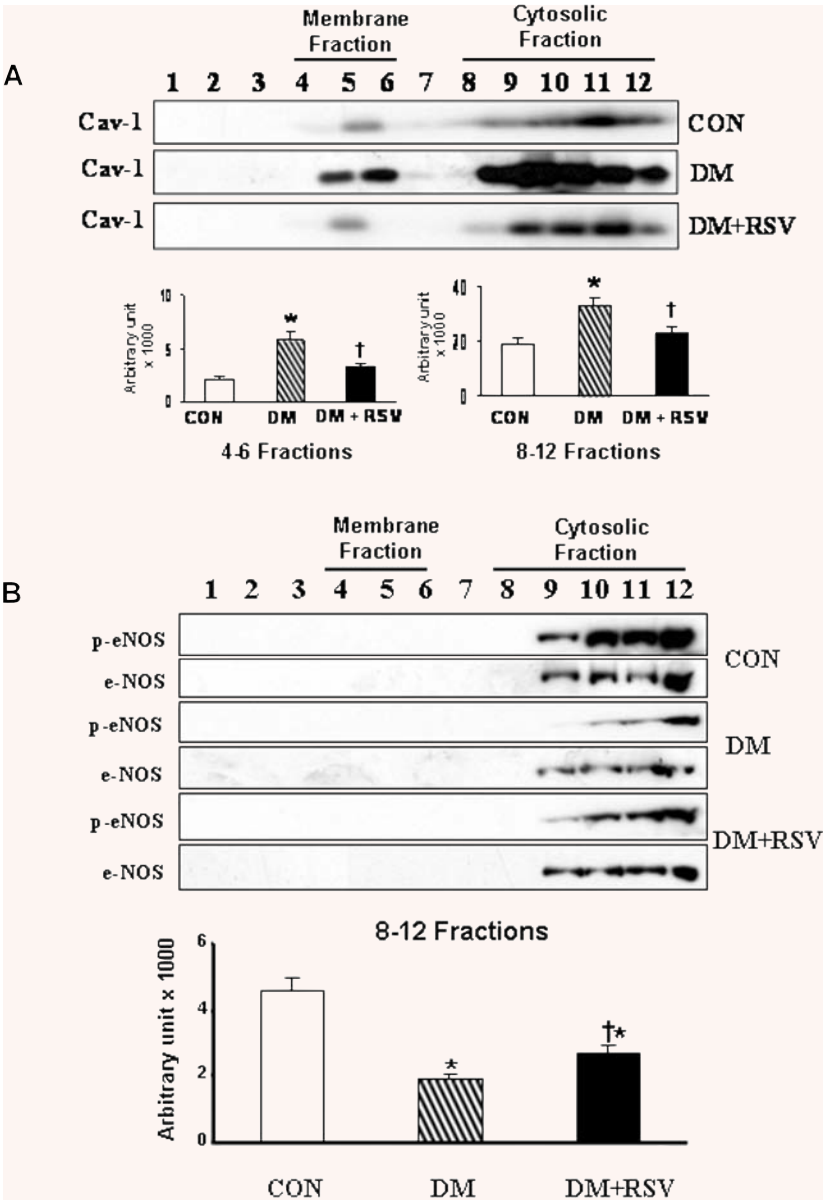

Fig. 3A and B Western blot represents the (**A**) caveolin-1 protein expression and (**B**) p-eNOS, eNOS in caveolin/lipid raft fractions in control, DM and DM+RSV groups. Fractions 4–6 represent the membrane fractions and 8–12 represent the cytosolic fractions. Graphs represent the quantitative expression between the groups. n = 6 times repeated experiments with equivalent results. $^{*}P < 0.05$ represent significant difference compared with control. $^{\dagger}P < 0.05$ represent significant difference compared with DM.

Effect of resveratrol on caveolin-1 and p-eNOS

Caveolin-1 level was found to be decreased under RSV treatment both in membrane (fractions 4–6) and cytosolic (fractions 8–12) fractions when compared to DM (Fig. 3A). Decreased phosphorylation of eNOS was observed in the diabetic group as compared to control group. RSV treatment increased the phosphorylation of eNOS (1.5-fold) as compared to DM group (Fig. 3B).

Effect of resveratrol on caveolin-3 and Glut-4 expression

In contrast to caveolin-1 expression, caveolin-3 expression was found to be increased in RSV when compared to diabetic group (Fig. 4A). Caveolin-3 expression was increased both in membrane (fractions 4–6) and cytosolic fractions (fractions 8–12) under RSV treatment that is decreased in diabetic group. RSV treatment increased the expression of Glut-4 in membrane as well as cytosolic fractions when compared to DM. Increased Glut-4 in the membrane

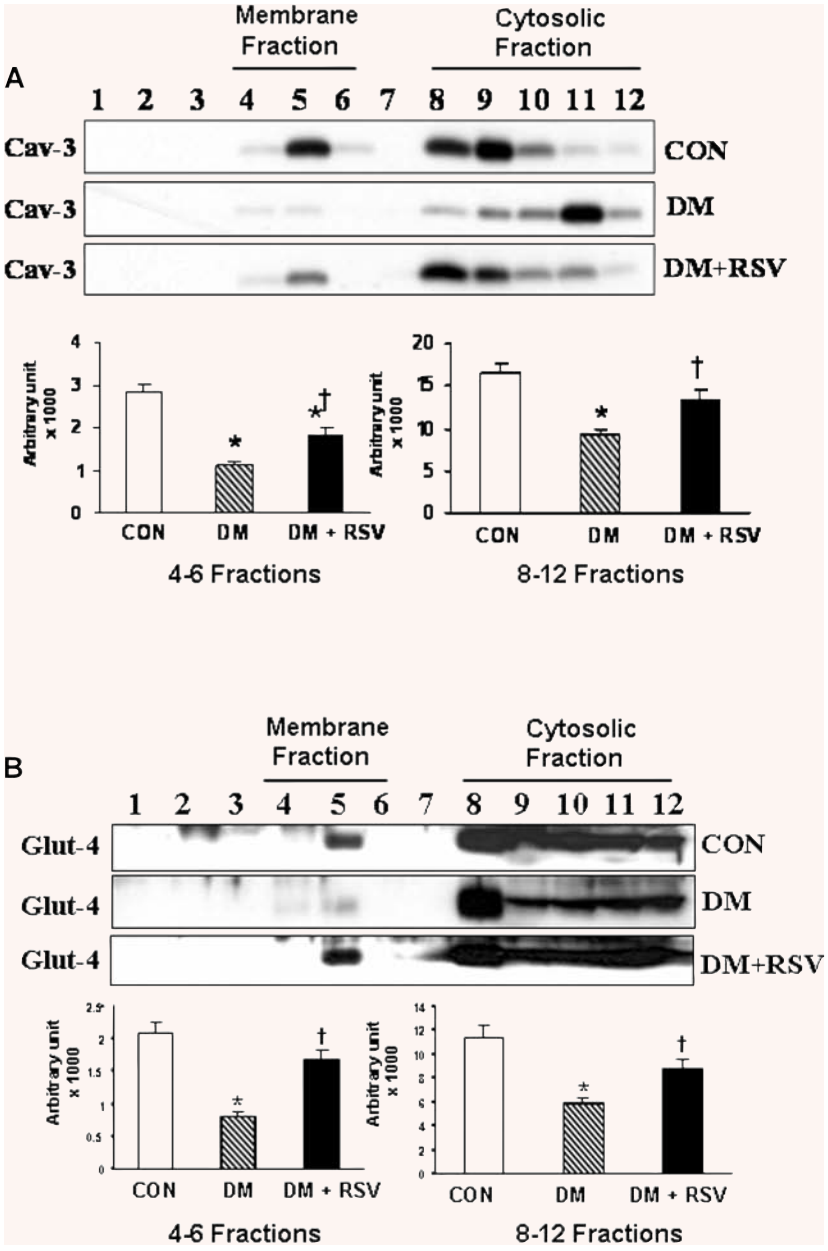

Fig. 4A and B Western blot represents the (**A**) caveolin-3 and (**B**) Glut-4 protein expression in caveolin/lipid raft fractions in control, DM and DM+RSV groups. Fractions 4–6 represent the membrane fractions and 8–12 represent the cytosolic fractions. Graphs represent the quantitative expression between the groups. n = 6 in each group. $^{*}P < 0.05$ represent significant difference compared with control. $^{\dagger}P < 0.05$ represent significant difference compared with DM.

fraction in RSV group might be due to increased translocation of Glut-4 following RSV treatment. Decreased expression of Glut-4 was observed both in membrane as well as cytosolic fractions in the DM compared to non-diabetic control group (Fig. 4B).

Effect of resveratrol on Caveolin-3/Glut-4 and Caveolin-1/eNOS association

Immunoprecipitation assay was performed to show the association of caveolin-3/Glut-4 and caveolin-1/eNOS in the caveolar-rich fractions (fractions 4–6) during diabetes. Decreased association of Glut-4 and Cav-3 was observed in diabetic group as compared to control group (Fig. 5A). RSV treatment documented increased association of Glut-4 and Cav-3 as compared to DM. The increased Glut-4 translocation and its association with Cav-3 on RSV treatment might have resulted in increased glucose uptake. Immunoprecipitation of Cav-1 and immunoblotting with eNOS clearly demonstrated that in diabetic group eNOS is significantly associated with Cav-1 as shown in Figure 5B. During RSV treatment we have observed dissociation of Cav-1 and eNOS that might have resulted in increased phosphorylation of eNOS.

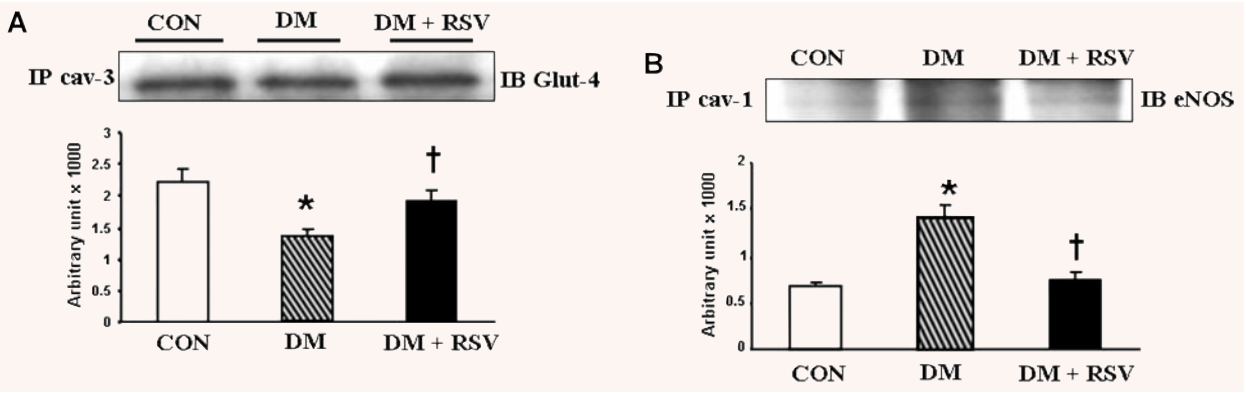

Fig. 5 (**A**) Immunoprecipitation with caveolin-3 and re-blot with Glut-4 in control, DM and DM+RSV groups. (**B**) Immunoprecipitation with caveolin-1 and re-blot with eNOS in control, DM and DM+RSV groups. n = 6 in each group. $P < 0.05$ represent significant difference compared with control. $^{\dagger}P < 0.05$ represent significant difference compared with DM.

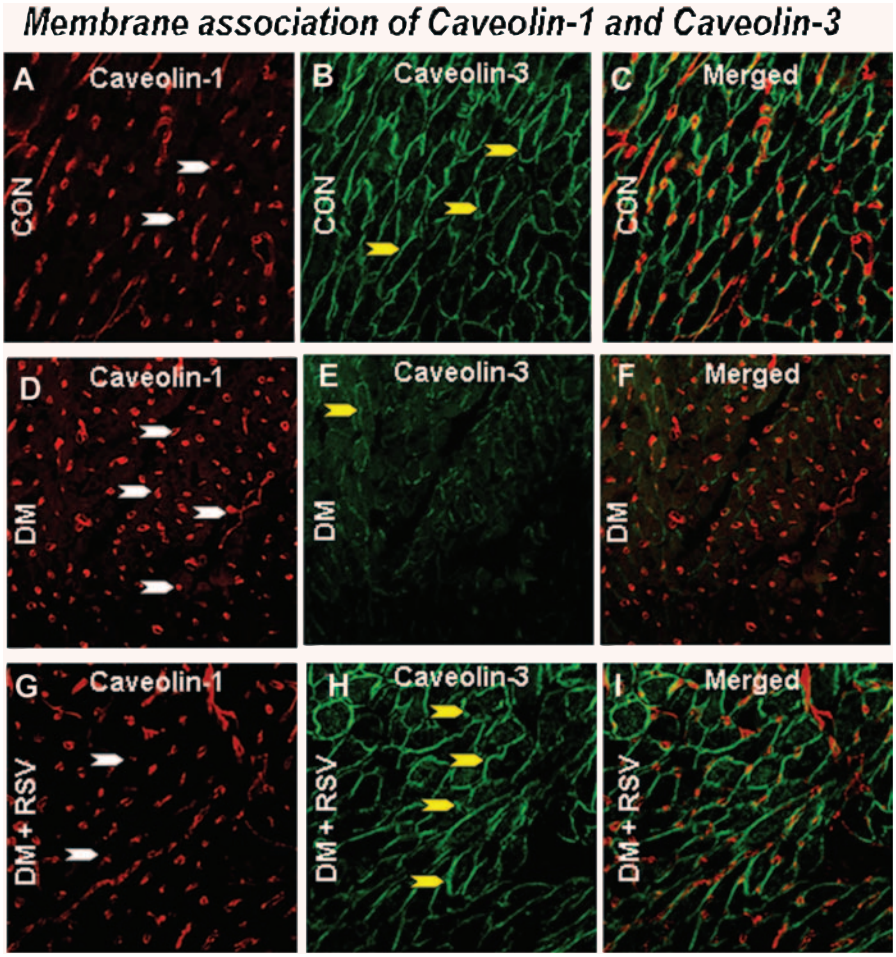

Fig. 6 Represents the rat cardiac paraffin sections labelled with immunofluorescence and visualized using confocal microscopy in control, DM and DM+RSV groups. A, D and G represent red fluorescence labelled caveolin-1. B, E and H represent the green fluorescence labelled caveolin-3. C, F and I represent the merged photo of Cav-1 and Cav-3. White arrows denote caveolin-1; Yellow arrows denote caveolin-3. The number of arrows represents the extent of expression of either Cav-1 or Cav-3. No significant co-localization (merged) was observed between the caveolin-1 and caveolin-3. n = 6 in each group.

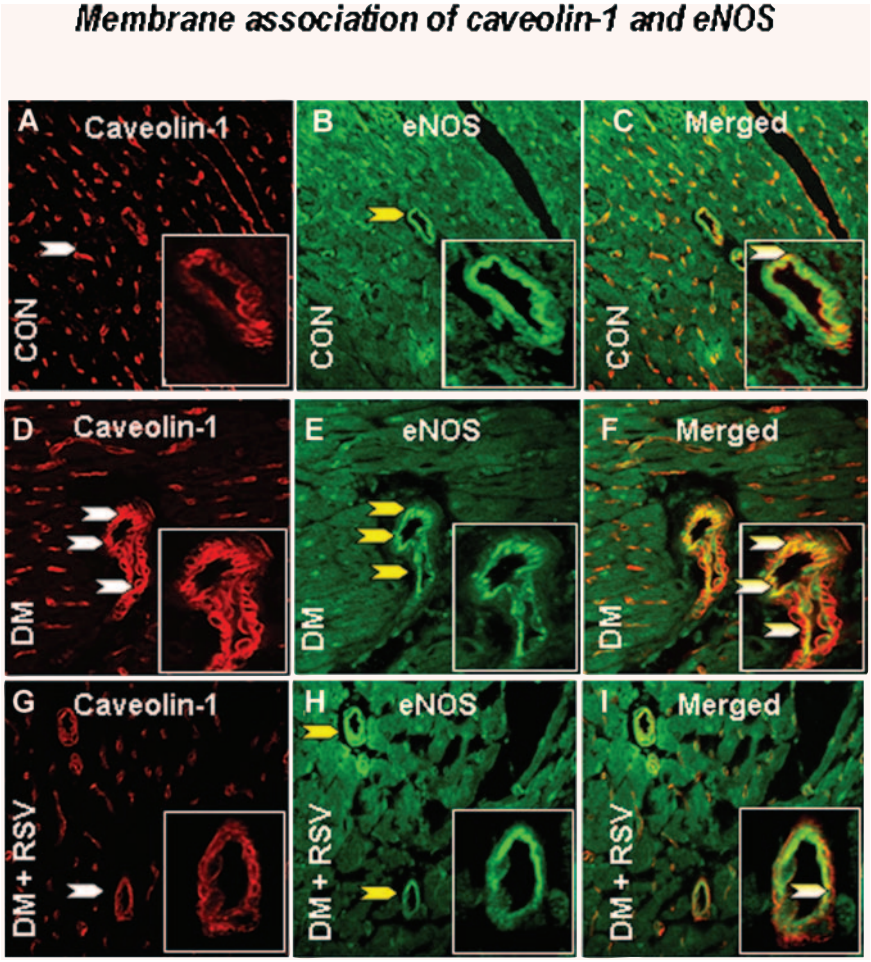

Fig. 7 Represents the rat cardiac paraffin sections labelled with immunofluorescence and visualized using confocal microscopy in control, DM and DM+RSV groups. A, D and G represent red fluorescence labelled caveolin-1. B, E and H represent the green fluorescence labelled eNOS. C, F and I represent the merged photo which clearly shows the co-localization of caveolin-1 / eNOS. n = 6 in each group. White arrows denote Caveolin-1, yellow arrows denote eNOS and the white/yellow (merged) arrow denotes the caveolin-1 and eNOS association / co-localization. The number of arrows represents the extent of expression of either cav-1, eNOS or the extent of co-localization. The figure in the box represents the magnified image demonstrating the co-localization.

Reduced eNOS phosphorylation in diabetic group as compared to control might be due to increased Cav-1/eNOS interaction or association that possibly made eNOS unavailable for its activation.

Immunohistochemical analysis of Cav-1/Cav-3, Cav-1/eNOS and Cav-3/Glut-4 association

Immunohistochemical analysis is shown in Figs 6–8 respectively. The immunohistochemical analysis documented significant increase in the expression of Cav-1 (stained in red in Fig. 6D) and decrease in the Cav-3 (stained in green in Fig. 6E) in the membrane of DM as compared to control. However, no significant co-localizaton of Cav-1/Cav-3 was observed in any of the groups (Fig. 6C, F and I). On treatment with RSV, decreased Cav-1 (Fig. 6G) expression and increased Cav-3 expression was observed (Fig. 6H) as expected. Significant association of Cav-1/eNOS in the membrane was observed in the diabetic group (Fig. 7F) as compared to control (Fig. 7C). On RSV treatment Cav-1/eNOS association was found to be decreased as compared to the diabetic group (Fig. 7I). DM has shown decreased Glut-4 translocation to the membrane and association with caveolin-3 (Fig. 8F) as compared to control (Fig. 8C). On RSV treatment, increased Glut-4 association with caveolin-3 was observed as compared to diabetic group (Fig. 8I).

Discussion

In the present study, we report hypoglycaemic effect of RSV and its role in regulation of myocardial Glut-4 translocation and glucose uptake in STZ-induced type-1 diabetic rats. This study shows that the RSV-mediated glucose uptake by modulating the Cav-1 and Cav-3 status in diabetic myocardium is mostly non-insulin related. We have observed increased translocation of Glut-4 and its association with caveolin-3 and dissociation of Cav-1/eNOS interaction in lipid raft fractions after RSV treatment. We have also documented increased phosphorylation of AMPK, eNOS and Akt on RSV treatment. From the results

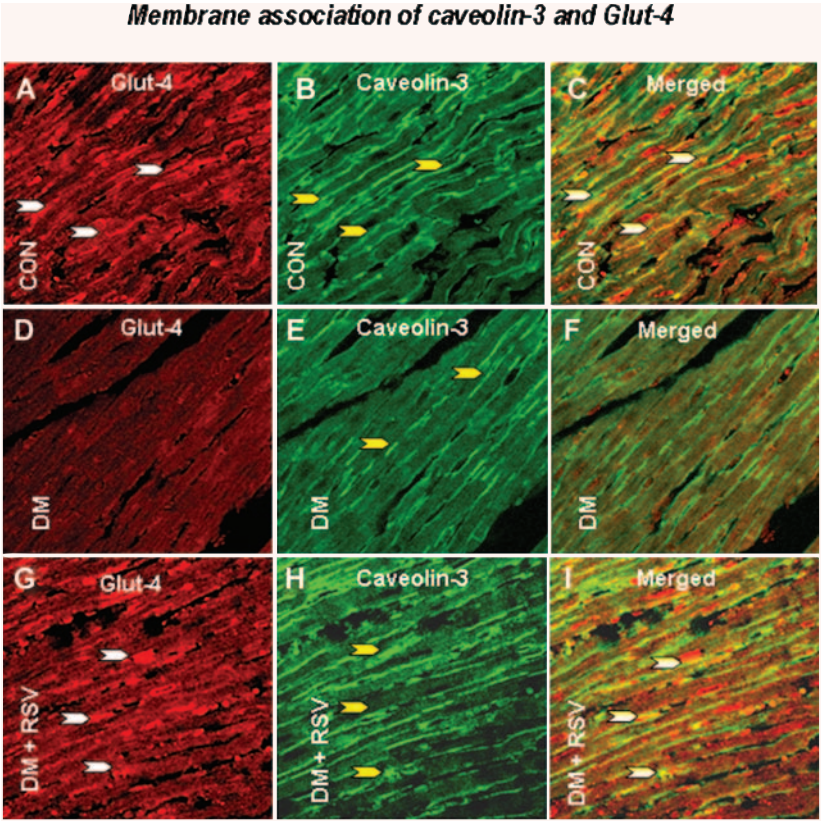

Fig. 8 Represents the rat cardiac paraffin sections labelled with immunofluorescence and visualized using confocal microscopy in control, DM and DM+RSV groups. A, D and G represent red fluorescence labelled Glut-4. B, E and H represent the green fluorescence labelled caveolin-3. C, F and I represent the merged photo that clearly shows the co-localization of caveolin-3 and Glut-4. n = 6 in each group. White arrows denote Glut-4, yellow arrows denote caveolin-3 and the white/yellow (merged) arrow denotes the caveolin-3 and Glut-4 association / co-localization. The number of arrows represents the extent of expression of either cav-3, Glut-4 or the extent of co-localization of cav-3/Glut-4.

obtained, we hypothesize that RSV-mediated Glut-4 translocation and glucose uptake might be AMPK /nitric oxide/ Akt mediated and regulated by caveolin-1 and caveolin-3 status which is independent of insulin signalling pathway. In addition, Chi *et al*. has also reported the reduction in glucose levels on treatment with RSV in which they demonstrated that RSV normalized hepatic phosphoenolpyruvate carboxykinase and increased Glut-4 expression in the soleus muscle of STZ diabetic rats [29] AMPK is a mediator of glucose metabolism [17] and is found to increase glucose transport by stimulating Glut-4 translocation to the sarcolemma in the heart [30]. It was previously reported that HepG2 cells treated with high glucose decreased phosphorylation of AMPK and its downstream target acetyl-CoA carboxylase (ACC) [31] and activation of AMPK by AICAR increased the translocation of Glut-4 in skeletal muscle [32]. Nitric oxide is a biological messenger synthesized in mammalian cells and nitric oxide- dependent glucose transport in skeletal muscle was reported after exercise-stimulation [33]. In addition, it is shown that activated AMPK phosphorylates eNOS on Ser^{1177} residue leading to NOS activation [34]. We have observed increased phosphorylation of AMPK as well as eNOS on RSV treatment as compared to diabetic group. At the basal level, eNOS is located within the plasma membrane microdomain caveolae and is negatively regulated by Cav-1. It acts as a physiological inhibitor of eNOS [35] and Gustavsson *et al*. has reported that during activation of endothelial cells the caveolin-1 inhibitory clamp is diminished by the recruitment of several proteins that promote an activation complex [36]. Bucci *et al*. has demonstrated a significant increase in the expression of Cav-1 in non-obese diabetic mice [11]. In skeletal muscle of eNOS knockout mice, diminished insulin stimulated glucose uptake was shown indicating the role of nitric oxide in glucose uptake [37].

In our present study, we have observed an increased expression of Cav-1 in DM as compared to the control. However, there was a subsequent decrease in Cav-1 expression upon RSV treatment in the diabetic group. Moreover, immunoprecipitation of Cav-1 from the membrane lipid raft fractions and re-blotting for eNOS showed an increased Cav-1/eNOS association in the diabetic group which was further evident from the reduced expression of phosphorylated eNOS in the heavier cytosolic fractions in the diabetic group as compared to the control. Upon RSV treatment we have observed reduced Cav-1/eNOS association and increased phosphorylation of eNOS in the diabetic group. Moreover, we have observed an increased activation of AMPK in RSV treated group as compared to the diabetic group. Therefore our data suggests that during diabetes there is an increased association of Cav-1/eNOS in the lipid rafts that makes eNOS unavailable for phosphorylation, but RSV treatment alleviates the Cav-1/eNOS association, thereby releasing more eNOS into the cytosol where it is phosphorylated by the active AMPK, thus rendering eNOS more active in the treated myocardium.

We recently reported that increased nitric oxide production during ischaemic preconditioning result in membrane translocation of Glut-4 and its association with Cav-3 [26]. As expected, we have also observed increased Glut-4 translocation and its association with Cav-3 upon RSV treatment as compared to STZ-induced DM. We have also observed increased expression of Cav-3 in RSV, and expression of Cav-3 was found to be necessary for the activation of PI3-kinase and Akt [38]. Reduced activation of both PI3-kinase and Akt in cells lacking Cav-3 expression has been reported [38]. In addition, we have observed increased activation of Akt in RSV-treated group as compared to DM. It is known fact that insulin-induced translocation of Glut-4 to the surface involves different signalling pathways like phosphorylation of insulin receptor substrate-1, activation of PI3 kinase and serine/threonine kinases like PKC and Akt/PKB [39]. Although the precise role of Akt/PKB action in Glut-4 translocation remains to be determined, reports show that phosphorylation and activation of Akt play an essential role in insulin-stimulated Glut-4 translocation by involvement in docking and / or fusion of Glut-4-containing vesicles with the cell surface [40]. It is recently reported that PI3 kinase is involved in the antihyperglycaemic effect of RSV and further demonstrated RSV induced Akt phosphorylation is inhibited by PI3 kinase inhibitors suggesting the role of activation of Akt in Glut-4 translocation and reduced glucose uptake [29]. Glut-4 translocation and insertion into the plasma membrane has been reported in adipocytes following Akt activation [41]. RSV-mediated activation of Akt might have also played a significant role in Glut-4 translocation and activation of glucose uptake.

Thus, our result suggests that the effect of RSV is non-insulin dependent and triggers some of the similar intracellular insulin signalling components in myocardium such as eNOS, Akt through AMPK pathway and also by regulating the caveolin-1 and caveolin-3 status that might play an essential role in Glut-4 translocation and glucose uptake in STZ- induced type-1 diabetic myocardium.

Acknowledgement

This study was supported by National Institutes of Health Grants HL 56803, HL 69910 and HL 85804.

References

1. **Berger J, Biswas C, Vicario PP, Strout HV, Saperstein R, Pilch PF.** Decreased expression of the insulin responsive glucose transporter in diabetes and fasting. *Nature.* 1989; 340: 70–2.
2. **Garvey WT, Huecksteadt TP, Birnbaum MJ.** Pretranslational suppression of an insulin-responsive glucose transporter in rats with diabetes mellitus. *Science.* 1989; 245: 60–3.
3. **Nikolaidis LA, Sturzu A, Stolarski C, Elahi D, Shen YT, Shannon RP.** The development of myocardial insulin resistance in conscious dogs with advanced dilated cardiomyopathy. *Cardiovascular Research.* 2004; 61: 297–306.
4. **Bryant NJ, Govers R, James DE.** Regulated transport of the glucose transporter Glut4. *Nat Rev Mol Cell Biol.* 2002; 3: 267–77.
5. **Gustavsson J, Parpal S, Stralfors P.** Insulin-stimulated glucose uptake involves the transition of glucose transporters to a caveolin rich fraction within the plasma membrane: implications for Type II diabetes. *Mol Med.* 1996; 2: 367–72.
6. **Anderson RG.** The caveolae membrane system. *Annu Rev Biochem.* 1998; 67: 199–225.
7. **Smart EJ, Graf GA, McNiven MA, Sessa WC, Engelman JA, Scherer PE, Okamoto T, Lisanti MP.** Caveolins, liquid ordered domains and signal transduction. *Mol Cell Biol.* 1999; 19: 7289–304.
8. **Parton RG.** Caveolae and caveolins. *Curr Opin Cell Biol.* 1996; 8: 542–8.
9. **Fleming I, Busse R.** Signal transduction of eNOS activation. *Cardiovasc Res.* 1999; 43: 532–41.
10. **Park H, Go YM, Darji R, Choi JW, Lisanti MP, Maland MC, Jo H.** Caveolin-1 regulates shear stress-dependent activation of extracellular signal-regulated kinase. *Am J Physiol Heart Circ Physiol.* 2000; 278: H1285–93.
11. **Bucci M, Roviezzo F, Brancaleone V, Lin MI, Lorenzo AD, Cicala C, Pinto A, Sessa WC, Farneti S, Fiorucci S, Cirino G.** Diabetic mouse angiopathy is linked to progressive sympathetic receptor deletion coupled to an enhanced caveolin-1 expression. *Arterioscler Thromb Vasc Biol.* 2004; 24: 721–6.
12. **Kapur S, Bedard S, Marcotte B, Cote C, Marette A.** Expression of nitric oxide synthase in skeletal muscle: a novel role for nitric oxide as a modulator of insulin action. *Diabetes.* 1997; 46: 1691–700.
13. **Kingwell BA, Formosa M, Muhlmanna M, Bradley SJ, McConell GK.** Nitric oxide synthase inhibition reduces glucose uptake during exercise in individuals with type 2 diabetes more than in control subjects. *Diabetes.* 2002; 51: 2572–80.
14. **Roberts CK, Barnard RJ, Scheck SH, Balon TW.** Exercise-stimulated glucose transport in skeletal muscle is nitric oxide dependent. *Am J Physiol Endocrinol Metab.* 1997; 36: E220–5.
15. **Rutter GA, Da Silva Xavier G, Leclerc I.** Roles of 5'-AMP-activated protein kinase (AMPK) in mammalian glucose homeostasis. *Biochem J.* 2003; 375: 1–16.
16. **Chen ZP, Mitchelhill KI, Michell BJ, Stapleton D, Crespo IR, Witters LA, Power DA, Ortiz de Montellano PR, Kemp BE.** AMP-activated protein kinase phosphorylation of endothelial NO synthase. *FEBS Letters.* 1999; 443: 285–9.
17. **Li J, Xu H, Selvakumar P, Russell RR, Cushman SW, Holman GD, Young LH.** Role of nitric oxide pathway in AMPK-mediated glucose uptake and Glut-4 translocation in heart muscle. *Am J Physiol Endocrinol Metab.* 2004; 287: E834–41.
18. **Thirunavukkarasu M, Penumathsa SV, Srikanth Koneru, Juhasz B, Zhan L, Otani H, Bagchi D, Das DK, Maulik N.** Resveratrol alleviates cardiac dysfunction in streptozotocin-induced diabetes: Role of nitric oxide, thioredoxin and heme oxygenase. *Free Rad Biol Med.* 2007; 43: 720–9.

19. **Penumathsa SV, Thirunavukkarasu M, Koneru S, Juhasz B, Zhan L, Pant R, Menon VP, Otani H, Maulik N.** Statin and resveratrol in combination induces cardioprotection against myocardial infarction in hypercholesterolemic rat. *J Mol Cell Cardiol.* 2007; 42: 508–16.
20. **Jager U, Nguyen-Duong H.** Relaxant effect of trans-resveratrol on isolated porcine coronary arteries. *Arzneimittelforschung.* 1999; 49: 207–11.
21. **Hattori R, Otani H, Maulik N, Das DK.** Pharmacological preconditioning with resveratrol: role of nitric oxide. *Am J Physiol Heart Circ Physiol.* 2002; 282: H1988–95.
22. **Lu R, Serrero G.** Resveratrol, a natural product derived from grape, exhibits antiestrogenic activity and inhibits the growth of human breast cancer cells. *J Cell Physiol.* 1999; 179: 297–304.
23. **Hung LM, Chen JK, Huang SS, Lee RS, Su MJ.** Cardioprotective effect of resveratrol, a natural antioxidant derived from grapes. *Cardiovasc Res.* 2000; 47: 549–55.
24. **Rotondo S, Rajtar G, Manarini S, Celardo A, Rotillo D, de Gaetano G, Evangelista V, Cerletti C.** Effect of trans-resveratrol, a natural polyphenolic compound on human polymorphonuclear leukocyte function. *Br J Pharmacol.* 1998; 123: 1691–9.
25. **Jang M, Cai L, Udeani GO, Slowing KV, Thomas CF, Beecher CW, Fong HH, Farnsworth NR, Kinghorn AD, Mehta RG, Moon RC, Pezzuto JM.** Cancer chemopreventive activity of resveratrol, a natural product derived from grapes. *Science.* 1997; 275: 218–20.
26. **Koneru S, Penumathsa SV, Thirunavukkarasu M, Samuel SM, Zhan L, Han Z, Maulik G, Das DK, Maulik N.** Redox regulation of ischemic preconditioning is mediated by the differential activation of caveolins and their association with eNOS and glut-4. *Am J Physiol Heart Circ Physiol.* 2007; 292: 2060–72.
27. **Kotani K, Ogawa W, Matsumoto M, Kitamura T, Sakaue H, Hino Y, Miyake K, Sano W, Akimoto K, Ohno S, Kasuga M.** Requirement of atypical protein kinase Cλ for insulin stimulation of glucose uptake but not for Akt activation in 3T3-L1 adipocyte. *Mol Cell Biol.* 1998; 18: 6971–82.
28. **Liu Y, Casey L, Pike LJ.** Compartmentalization of phosphatidylinositol 4,5-biphosphate in low-density membrane domains in the absence of caveolin. *Biochem Biophys Res Commun.* 1998; 245: 684–90.
29. **Chi TC, Chen WP, Chi TL, Kuo TF, Lee SS, Cheng JT, Su MJ.** Phosphotidylinositol-3-kinase is involved in the antihyperglycemic effect induced by resveratrol in streptozotocin –induced diabetic rats. *Life Sci.* 2007; 80: 1713–20.
30. **Russell RR, Bergeron R, Shulman GI, Young LH.** Translocation of myocardial glut4 and increased glucose uptake through activation of AMPK by AICAR. *Am J Physiol Heart Circ Physiol.* 1999; 277: H643–9.
31. **Dyck JRB, Kudo N, Barr AJ, Davies SP, Hardie DG, Lopaschuk GD.** Phosphorylation control of cardiac acetyl-coA carboxylase by cAMP-dependent protein kinase and 5'-AMP activated protein kinase. *Eur J Biochem.* 1999; 262: 184–90.
32. **Kurth-Kraczek EJ, Hirshman MF, Goodyear LJ, Winder WW.** 5´ AMP-activated protein kinase activation causes glut-4 translocation in skeletal muscle. *Diabetes.* 1999; 48: 1667–71.
33. **Roberts CK, Barnard RJ, Scheck SH, Balon TW.** Exercise-stimulated glucose transport in skeletal muscle is nitric oxide dependent. *Am J Physiol Endocrinol Metab.* 1997; 273: E220–5.
34. **Morrow VA, Foufelle F, Connell JM, Petrie JR, Gould GW, Salt IP.** Direct activation of AMP-activated protein kinase stimulates nitric oxide synthesis in human aortic endothelial cells. *J Biol Chem.* 2003; 278: 31629–39.
35. **Garcia-Cardena G, Martasek P, Master BS, Skidd PM, Couet J, Li S, Lisanti MP, Sessa WC.** Dissecting the interaction between nitric oxide snythase (NOS) and caveolin. Functional significance of the NOS caveolin binding domain *in vivo. J Biol Chem.* 1997; 272: 25437–70.
36. **Gustavsson J, Parpal S, Karlsson M, Ramsing C, Thorn H, Borg M, Lindroth M, Peterson KH, Magnusson KE, Stralfors P.** Localization of the insulin receptor in caveolae of adipocyte plasma membrane. *FASEB J.* 1999; 13: 1961–71.
37. **Duplain H, Burcelin R, Sartori C, Cook S, Egli M, Lepori M, Vollenweider P, Pedrazzini T, Nicod P, Thorens B, Scherrer U.** Insulin resistance, hyperlipidemia, and hypertension in mice lacking endothelial nitric oxide synthase. *Circulation.* 2001; 104: 342–5.
38. **Fecchi K, Volonte D, Hezel MP, Schmeck K, Galbiati F.** Spatial and temporal regulation of glut-4 translocation by flotillin-1 and caveolin-3 in skeletal muscle cells. *FASEB J.* 2006; 20: 705–7.
39. **Alessi DR, James SR, Downes CP, Holmes AB, Gaffney PRJ, Reese CB, Cohen P.** Characterization of a 3-phosphoinositide–dependent protein kinase which phosphorylates and activates protein kinase Bα. *Current Biol.* 1997; 7: 261–9.
40. **Ducluzeau PH, Fletcher LM, Welsh GI, Tavare JM.** Functional consequence of targeting protein kinase B/ Akt to Glut4 vesicles. *J Cell Sci.* 2002; 115: 2857–66.
41. **Cong LN, Chen H, Li Y, Zhou L, McGibbon MA.** Physiological role of Akt in insulin stimulated translocation of Glut4 in transfected rat adipose cells. *Mol Endocrinol.* 1997; 11: 1881–90.